A Continuous Approach to Minimize Cost for Charging Electric Bus Fleets

Daniel Mortensen, Jacob Gunther, Greg Droge, Alexander Brown, Justin Whitaker

***Abstract*—**

***Index Terms*—Battery Electric Buses, Cost Minimization, Multi-Rate Charging, Mixed Integer Linear Program**

I. Introduction

Battery powered electric motors for buses have long been a desired alternative to the internal combustion engine [18]. The reduced maintenance [1], zero emissions [15], and access to renewable energy [7] are but some of the benefits that have caused transit authorities to begin incorporating them into their bus fleets.

Despite their benefits, transitioning to battery electric buses (BEBs) must address additional challenges, in particular, their extended refuel times. If a diesel or CNG bus runs low on fuel, refueling takes five to ten minutes. An electric bus on the other hand may require several hours, causing the bus to fall behind schedule.

Maintaining a schedule while staying charged is one of the main challenges that BEBs face, and requires careful planning which must account for the battery discharge along routes, charge times, and a limited number of chargers.

Charging while a bus is in motion, or dynamic charging, is one way to simplify a charge plan. There are a number of ways to do this including overhead [8] and inductive charging [14] [4]. An overhead charging scenario allows the bus to charge on overhead power lines while in motion while inductive charging relies on specialized hardware in the roads to inductively transfer energy when a bus passes overhead. Both methods remove the need to stop for service and allow an electrical vehicle to stay in service indefinitely. They also require extensive infrastructure [2] that may not be available.

In the absence of infrastructure, [13] and [30] have proposed methods that exchange depleted batteries for fresh ones. Such a method would eliminate both the logistical challenges of planning and the infrastructure dependence of dynamic charging. The only drawback, is that BEBs are not built with battery exchanges in mind, therefore the task can require specialized hardware, technical expertise, or automation, all of which add complexity and cost.

One charge option that avoids both the infrastructural demands of dynamic charging and the technical difficulties of battery swapping is stationary charging, which plans rest periods into a bus's schedule during which that bus can charge [29]. Stationary charging is the least invasive form of bus charging because it only requires charging hardware at specific locations and makes no exchanges to bus batteries. Prior work in this area addresses a number of problems including distributed charging networks [20], bus availability, environmental impact [31], route scheduling [24], battery health [12], the cost of electricity [16] and the cost of charging infrastructure [28].

One drawback to using a stationary charging solution is that it does require significant rest periods for charging. One way to decrease the charge intervals is to use high power chargers, which deliver more energy in a smaller period of time. Large power demands however do increase the overall cost of energy because they must be supported by highly capable infrastructure [26], [9], [5]. An effective charge plan must therefore balance the need to charge quickly with the desire to maintain a low power profile [7], [21], [23], [3], [27], [11] which includes power used by BEBs and the power needed by other consumers.

Because the additional power users are outside the control of the charge plan, their power requirements are referred to in this paper as “uncontrolled loads”. Uncontrolled loads complicate the problem of finding an optimal charge plan. If a bus charges in the presence of a large uncontrolled load, the overall power profile rises, increasing cost for energy.

A significant contribution of [19] was how the authors minimized the the financial impact of charging in the presence of uncontrolled loads by formulating the charge problem as a network flow on a graph and solving for the optimal path through the graph. The graph-based approach represented time discretely, which lent itself well to integrating uncontrolled loads, which are sampled discretely in practice.

Unfortunately, more temporal precision decreases the time step between sections in the graph, which leads to a larger graph and significantly increases the computational complexity. The authors of [6] compute the charge schedule continuously by formulating the charge problem as a bin packing problem [17], yielding a precise time schedule for charging, but finding a continuous-time schedule that incorporates uncontrolled loads and minimizes a comprehensive cost function remains an open problem and is the focus of this paper.

The rest of this paper is organized as follows: Section II discuses the basic problem formulation, Section III discuses linear constraints that govern the behavior and limitations of the sate of charge. Section IV discuses how to incorporate uncontrolled loads into the optimization framework. Section V explains how the objective function is formed, and Section VI discusses performance.

II. Availability and Resource Contention

The charge scheduling framework described in this paper is formulated as a constrained optimization problem that can be solved as a Mixed Integer Linear Program (MILP) of the form

$$\begin{aligned} &\min_{\mathbf{y}} \mathbf{y}^T \mathbf{v} \text{ subject to} \\ &\tilde{A}\mathbf{y} = \tilde{\mathbf{b}},\ A\mathbf{y} \leq \mathbf{b}, \end{aligned} \tag{1}$$

where $\mathbf{y}$, $\tilde{A}$, A, and $\mathbf{g}$ represent the solution vector, equality and inequality constraints, and cost vector respectively. In this paper, $\mathbf{y}$ is comprised of several variables, and is expressed as

$$\mathbf{y} = \begin{bmatrix} \boldsymbol{\sigma} \\ \mathbf{c} \\ \mathbf{s} \\ \mathbf{h} \\ \mathbf{k} \\ \mathbf{r} \\ \mathbf{g} \\ \mathbf{p} \\ q_{\text{on}} \\ q_{\text{all}} \end{bmatrix}, \tag{2}$$

where $\boldsymbol{\sigma}$ describes on which charger a bus will charge, $\mathbf{c}$ and $\mathbf{s}$ describe time intervals over which buses charge, $\mathbf{h}$ gives the bus state of charge, $\mathbf{k}$, $\mathbf{r}$ and $\mathbf{p}$ are used to discretize the effects from $\mathbf{c}$ and $\mathbf{s}$, and q_{on} and q_{all} represent maximum average power values that are used to compute the monthly cost of power.

The cost function in (1) will be designed to model a realistic billing structure used by [22] and minimises the cost even in the presence of uncontrolled loads. Additionally, the constraints are designed to incorporate bus schedules, limit bus state of charges, and include a linear charge model calibrated on data from the Utah Transit Authority.

A. Setup

A solution to the bus charge problem includes both temporal and categorical information. The temporal aspect shows when and for how long a bus should charge and the categorical shows which bus must charge, indicating a solution with two dimensions. The first dimension represents time continuously from left to right, and the second describes the buses as shown in Fig. 1.

Each bus follows a schedule of arrival and departure times, where the i^{th} bus's j^{th} stop begins at arrival time a_{ij} and terminates at departure time d_{ij} (see Fig. 2). A bus can be assigned to charge anytime the bus is in the station such that the charge start time, c_{ij}, is greater than or equal to a_{ij}, and the charge stop time, s_{ij}, is less than the departure time d_{ij} as shown in Fig. 2. In the context of a MILP, the arrival and departure times a_{ij} and d_{ij} are known ahead of time and charge times c_{ij} and s_{ij} are optimization variables.

B. Constraints

The relationship between the arrival, departure, and charge intervals for the i^{th} bus at the j^{th} stop can be expressed as a set of inequality constraints such that

$$\begin{aligned} a_{ij} &< c_{ij} \\ c_{ij} &< s_{ij} \\ s_{ij} &< d_{ij}. \end{aligned} \tag{3}$$

These constraints can be rewritten such that the optimization variables are on the left, the known parameters are on the right, and the relationship is ”less than” (or standard form) such that

$$\begin{aligned} -c_{ij} &< -a_{ij} \\ c_{ij} - s_{ij} &< 0 \\ s_{ij} &< d_{ij}. \end{aligned} \tag{4}$$

Standard form is preferred because it provides a standard way to represent equations. Having the optimization variables on the left also allows the expression to be written using matrix notation as

$$\begin{bmatrix} -1 & 0 \\ 1 & -1 \\ 0 & 1 \end{bmatrix} \begin{bmatrix} c_{ij} \\ s_{ij} \end{bmatrix} \leq \begin{bmatrix} -a_{ij} \\ 0 \\ d_{ij} \end{bmatrix}. \tag{5}$$

However, because all constraints must follow the form $A\mathbf{y} = \mathbf{b}$ as shown in (1), (5) is expressed in terms of $\mathbf{y}$ such that

$$\begin{aligned} \begin{bmatrix} -1^c_{ij} & 0 & \dots & 0 \\ 1^c_{ij} & 0 & \dots & -1^d_{ij} \\ 0 & 0 & \dots & 1^d_{ij} \end{bmatrix} \mathbf{y} &\leq \begin{bmatrix} -a_{ij} \\ 0 \\ d_{ij} \end{bmatrix} \ \forall i,j \\ A_1\mathbf{y} &\leq \mathbf{b}_1, \end{aligned} \tag{6}$$

where 1^c_{ij} is 1 at the location corresponding to c_{ij}, 1^d_{ij} is 1 at the location corresponding to d_{ij}, and A_1 and $\mathbf{b}_1$ stack the constraints given in (5) for all i, j.

The decision variables s_{ij} and c_{ij} from (5) show when a bus must start and finish charging, but do not indicate on which charger. The variable $\boldsymbol{\sigma}$ from (2) is a vector of binary variables. Each element of $\boldsymbol{\sigma}$ is denoted σ_{ijk} and is 1 when bus i charges during the j^{th} stop at charger k. Because a bus can only charge at one charger at a time, the values in $\boldsymbol{\sigma}$ must be constrained such that

$$\sum_k \sigma_{ijk} \leq 1 \ \forall i,j \tag{7}$$

or in standard form as

$$\begin{aligned} \begin{bmatrix} 1_{ij1} & 0 & \dots & 0 & 1_{ijk} \end{bmatrix} \mathbf{y} &\leq \mathbf{1} \ \forall i,j \\ A_2\mathbf{y} &\leq \mathbf{b}_2, \end{aligned} \tag{8}$$

where 1_{ijk} represents a 1 at the location corresponding to σ_{ijk}. The variable σ_{ijk} is used in several scenarios. The first is to ensure that buses without charge assignments have a charge

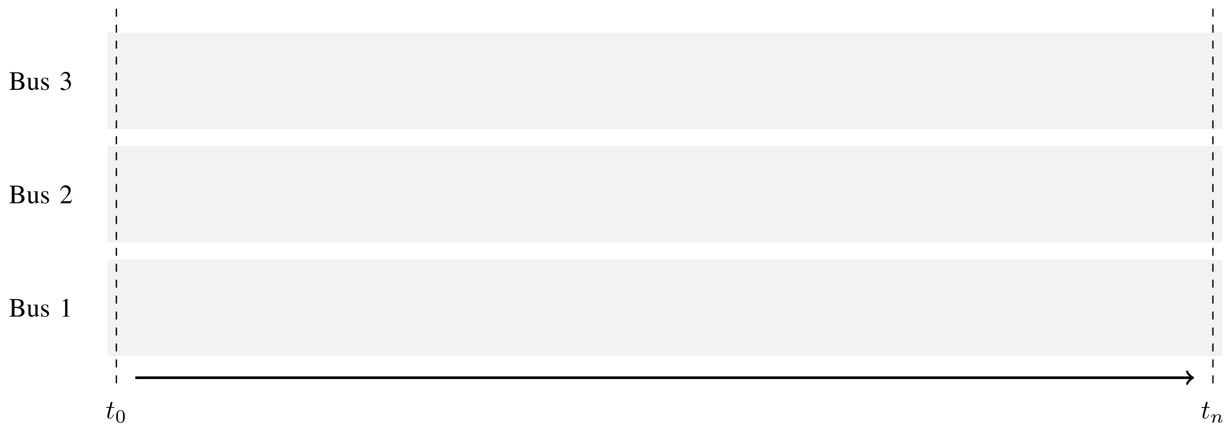

Fig. 1: Description of the bus and time axis

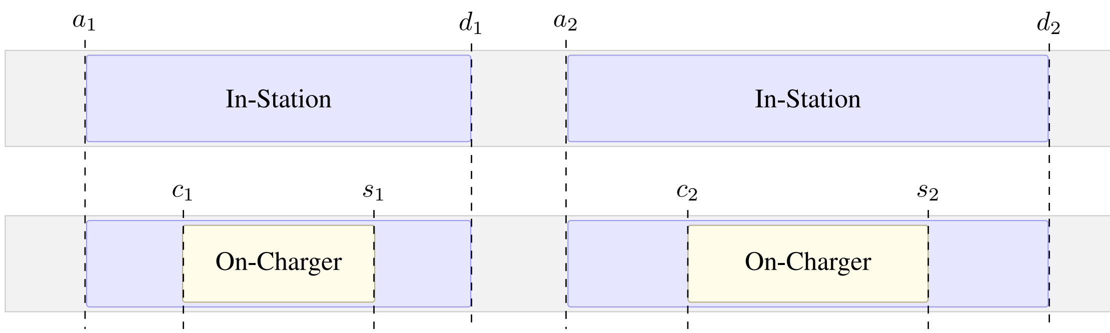

Fig. 2: Bus Charging

time of zero by constraining s_{ij} and c_{ij} to be the same value. This is done by letting

$$
\begin{gathered}
s_{ij} - c_{ij} \le M \sum_k \sigma_{ijk} \\
s_{ij} - c_{ij} - \sum_k \sigma_{ijk} M \le 0 \\
\begin{bmatrix} 1_s & -1_c & -M_\sigma \end{bmatrix} \begin{bmatrix} s_{ij} \\ c_{ij} \\ \sigma_{ij1} \\ \vdots \\ \sigma_{ijk} \end{bmatrix} \le 0 \; \forall i, j
\end{gathered}
\tag{9}
$$

where M is the maximum difference between s_{ij} and c_{ij}, or the number of seconds in a day, denoted nTime and M_σ represents multiple values of M at locations corresponding to each σ_{ijk}. The constraints in (9) can be appropriately zero padded and stacked for all i, j to form the linear expression

$$A_3 \mathbf{y} \le \mathbf{b}_3 \tag{10}$$

The values in $\boldsymbol{\sigma}$, $\mathbf{c}$, and $\mathbf{s}$ form a complete charge plan representation were c_{ij} and s_{ij} describe time periods when a bus will charge and σ_{ijk} gives which charger to use. (see Fig. 3). The variable σ_{ijk} is also necessary to eliminate situations where more then one bus is assigned to a charger at the same time. Note that this can only happen when a_{ij} for bus i is less than $d_{i' j'}$ for bus $i^{'}$ as shown in Fig. 4. Let $\mathcal{S}$ be the set of all bus break pairs such that $\left(ij,\ i^{`}j^{`}\right) \in \mathcal{S}$ if overlap is possible between bus i and bus $i^{`}$ during the $j$ and $j^{`}$ stops respectively. Charging overlap can be avoided by constraining

$$
\begin{array}{c} c_{i^{`}j^{`}} > s_{ij} \\ \text{or} \\ c_{ij} > s_{i^{`}j^{`}} \end{array} \quad \forall \left(ij,\ i^{`}j^{`}\right) \in \mathcal{S}
\tag{11}
$$

Let $l_{(ij,\ i^{`}j^{`})}$ be a binary decision variable that is 1 when $c_{i' j'} > s_{ij}$, and 0 when $c_{ij} > s_{i' j'}$. The expression from (11) can be rewritten as

$$
\begin{aligned}
c_{i^{`}j^{`}} - s_{ij} &> -M l_{(ij,\ i^{`}j^{`})} \\
c_{ij} - s_{i^{`}j^{`}} &> -M(1 - l_{(ij,\ i^{`}j^{`})})
\end{aligned}
\tag{12}
$$

However, this constraint is only necessary when buses i and $i^{`}$ must use the same charger. This can be remedied as

$$
\begin{aligned}
c_{i' j'} - s_{ij} &> M\left[(\sigma_{i' j' k} + \sigma_{ijk}) - 2\right] - M l_{(ij,\ i^{`}j^{`})} \; \forall k \\
c_{ij} - s_{i' j'} &> M\left[(\sigma_{i' j' k} + \sigma_{ijk}) - 2\right] - M(1 - l_{(ij,\ i^{`}j^{`})}) \; \forall k
\end{aligned}
\tag{13}
$$

When $(\sigma_{i' j' k} + \sigma_{ijk}) < 2$, (14) is trivially satisfied for all values of $c_{i' j'}$ and s_{ij}. When $\sigma_{i' j' k} = \sigma_{ijk} = 1$, (14) simplifies to (12). Equation (14) can be expressed in standard form as

$$
\begin{aligned}
-c_{i^{`}j^{`}} + s_{ij} + M\sigma_{i' j' k} + M\sigma_{ijk} - M l_{iji^{`}j^{`}} &\le 2M \; \forall k \\
-c_{ij} + s_{i^{`}j^{`}} + M\sigma_{i' j' k} + M\sigma_{ijk} + M l_{iji^{`}j^{`}} &\le 3M \; \forall k
\end{aligned}
\tag{14}
$$

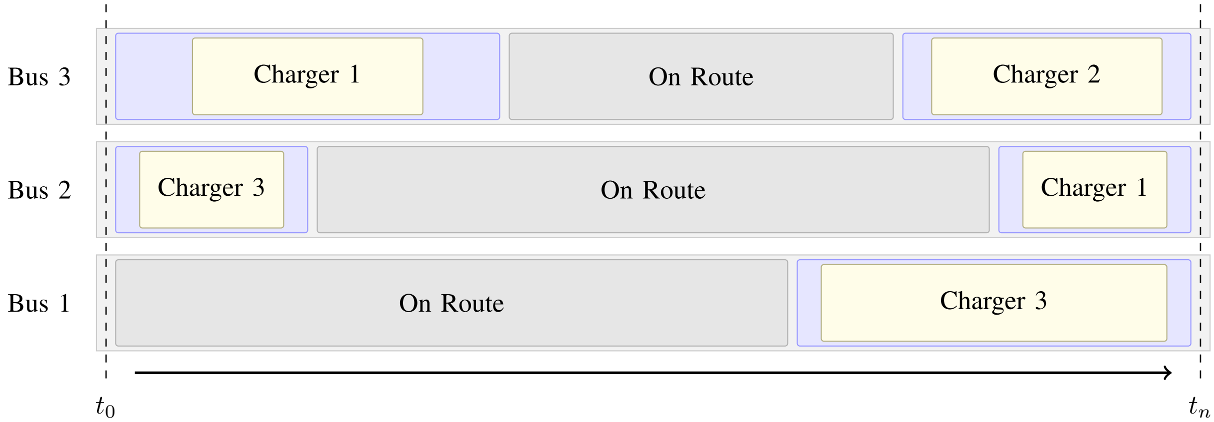

Fig. 3: Reserving time slots on chargers

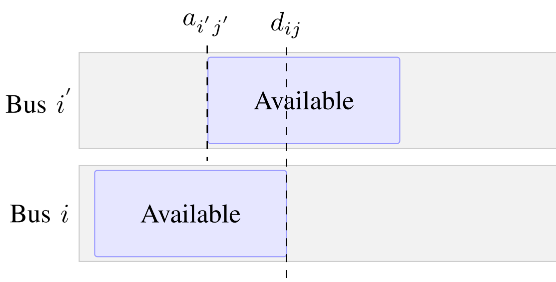

Fig. 4: Potential Overlap

and finally as

$$\begin{bmatrix} -1 & 0 & 0 & 1 & M & M & -M \\ 0 & 1 & -1 & 0 & M & M & M \end{bmatrix} \begin{bmatrix} c_{i'j'} \\ s_{i'j'} \\ c_{ij} \\ s_{ij} \\ \sigma_{i'j'k} \\ \sigma_{ijk} \\ l_{iji'j'} \end{bmatrix} \leq \begin{bmatrix} 2M \\ 3M \end{bmatrix} \forall k \tag{15}$$

The constraints in (14) can be repeated for all $\left(ij,\ i'j'\right) \in \mathcal{S}$ and concatenated into a single matrix expression

$$A_4 \mathbf{y} \leq \mathbf{b}_4 \tag{16}$$

III. Battery State of Charge

BEBs must also maintain their state of charge above a minimum threshold, denoted h_{min}. Let h_{ij} be the state of charge for bus i at the beginning of stop j as shown in figure 5. The initial value for bus i, denoted h_{i0}, is equal to some constant such that

$$\begin{gathered} h_{i0} = \eta_i \ \forall i \\ \begin{bmatrix} 0 & 0 & \dots & 0 & 1_i & 0 \end{bmatrix} \mathbf{y} = \eta_i \ \forall i \\ \tilde{A}_1 \mathbf{y} = \tilde{\mathbf{b}}_1 \end{gathered} \tag{17}$$

and is otherwise computed as the the sum of incoming and outgoing energy where incoming energy comes from charging, and outgoing energy comes from the battery discharge. The discharge from operating bus i over route j is denoted δ_{ij}. The increase in battery state of charge follows a linear charge model such that the increase is equal to the energy rate, denoted p_i, times the time spent charging, denoted Δ_{ij}[25]. The total change from h_{ij} to h_{ij+1} can be expressed as

$$h_{ij+1} = h_{ij} + \Delta_{ij} \cdot p_i - \delta_{ij}. \tag{18}$$

The value for Δ_{ij} can also be expressed in terms of the difference between a_{ij} and d_{ij} such that

$$\begin{gathered} h_{ij} + p_i \cdot (s_{ij} - c_{ij}) - \delta_i = h_{ij+1} \\ h_{ij+1} - h_{ij} - p_i s_{ij} + p_i c_{ij} = -\delta_i \\ \begin{bmatrix} 1 & -1 & -p_i & p_i \end{bmatrix} \begin{bmatrix} h_{ij+1} \\ h_{ij} \\ s_{ij} \\ c_{ij} \end{bmatrix} = -\delta_i \ \forall i,j \end{gathered} \tag{19}$$

The constraints for each i, j outlined in (19) can be vertically concatenated to form

$$\begin{gathered} A_{ij} \mathbf{y} = \mathbf{b}_{ij} \ \forall i,j \\ \tilde{A}_2 \mathbf{y} = \tilde{\mathbf{b}}_2 \end{gathered} \tag{20}$$

Now that the state of charge is defined, the next constraint ensures that the minimum battery state of charge remains both above the minimum threshold, h_{min}, and below the battery capacity, h_{max}. These constraints are given as

$$\left.\begin{aligned} -h_{ij} &\leq -h_{\text{min}} \\ h_{ij} &\leq h_{\text{max}} \end{aligned}\right. \quad \forall i,j \tag{21}$$

or

$$\begin{gathered} \begin{bmatrix} 0 & \dots & 0 & -1_h & 0 & \dots & 0 \\ 0 & \dots & 0 & 1_h & 0 & \dots & 0 \end{bmatrix} \mathbf{y} \leq \begin{bmatrix} h_{\text{min}} \\ h_{\text{max}} \end{bmatrix} \ \forall ij \\ A_5 \mathbf{y} \leq \mathbf{b}_5 \end{gathered} \tag{22}$$

The final constraint has to do with the assumption that we desire to use the model for one day to predict the expected cost over a month. To do this, the state of charge at the end of the day must equal the state of charge at the beginning. Let $h_{i,\text{end}}$ be the final daily state of charge for bus i. This is constrained to be the same as the beginning state of charge as

$$\begin{gathered} h_{i0} = h_{i,\text{end}} \ \forall i \\ h_{i0} - h_{i,\text{end}} = 0 \ \forall i. \end{gathered} \tag{23}$$

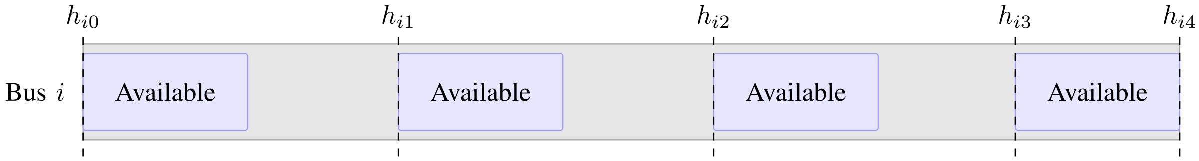

Fig. 5: State of Charge Variables

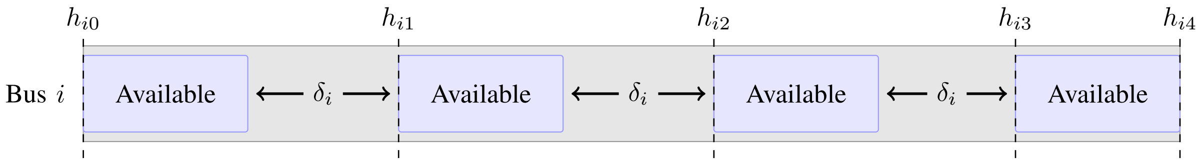

Fig. 6: Placement for δ_i

However, because equality for two continuous variables is computationally demanding, the constraint in (23) can also be expressed as

$$h_{i0} - h_{i,\text{end}} \leq 0. \tag{24}$$

Because the final state of charge is dependent on the amount of power used to charge, and power/energy use is penalized (see section V), the optimization process will force the final state of charge down until is nearly equal to the initial.

IV. Integrating Uncontrolled Loads

A monthly power bill is made up of several costs, two of which depend on the maximum energy consumed over 15 minutes. This 15-minute average power includes energy that is consumed by loads other than bus chargers, or ”uncontrolled loads”. In practice, data for uncontrolled loads is sampled and therefore discrete. The representations for how buses use power in Section III are continuous, making their effects difficult to integrate with a discrete uncontrolled load. This section integrates these uncontrolled loads into the planning framework by converting the continuous start and end points, c_{ij} and s_{ij} from section II, to a vector $\mathbf{p}_{ij}$, where the n^{th} element of $\mathbf{p}_{ij}$ represents the average power over the interval t_{i-1} to t_i from bus i during route j. These route power vectors can be added together to form a discrete profile for the buses.

Let the day be divided into time segments, each of duration ΔT. The first step is to determine the index of each segment that a bus begins charging, k_{ij}^{start}, and the index of the segement that a bus finishes charging, k_{ij}^{end}. Each index can be computed as an integer multiple of ΔT that satisfies

$$\begin{gathered}\left(k_{ij}^{\text{start}} - 1\right) \cdot \Delta T + r_{ij}^{\text{start}} = c_{ij} \\ \left(k_{ij}^{\text{end}} - 1\right) \cdot \Delta T + r_{ij}^{\text{end}} = s_{ij} \\ k_{ij}^{\text{start}}, k_{ij}^{\text{end}} \in \mathbb{Z} \\ 0 < r_{ij}^{\text{start}}, r_{ij}^{\text{end}} < \Delta T.\end{gathered} \tag{25}$$

Equation (25) yields the discrete indices k_{ij}^{start} and k_{ij}^{end} along with corresponding remainder values r_{ij}^{start} and r_{ij}^{end} which will be used later in this section to calculate the average power for time segments in which buses only charge part of the time. Equation (25) can be rewriten in standard form and zero padded such that

$$\begin{gathered}\begin{bmatrix} \Delta T & 1 & -1 & 0 & 0 & 0 \\ 0 & 0 & 0 & \Delta T & 1 & -1 \end{bmatrix} \begin{bmatrix} k_{ij}^{\text{start}} \\ r_{ij}^{\text{start}} \\ c_{ij} \\ k_{ij}^{\text{end}} \\ r_{ij}^{\text{end}} \\ s_{ij} \end{bmatrix} = \begin{bmatrix} 0 \\ 0 \end{bmatrix} \quad \forall i, j \\ \tilde{A}_2 \mathbf{y} = \tilde{\mathbf{b}}_2. \end{gathered} \tag{26}$$

and

$$\begin{gathered}\begin{bmatrix} 0 & -1 & 0 & 0 & 0 & 0 \\ 0 & 1 & 0 & 0 & 0 & 0 \\ 0 & 0 & 0 & 0 & -1 & 0 \\ 0 & 0 & 0 & 0 & 1 & 0 \end{bmatrix} \begin{bmatrix} k_{ij}^{\text{start}} \\ r_{ij}^{\text{start}} \\ c_{ij} \\ k_{ij}^{\text{end}} \\ r_{ij}^{\text{end}} \\ s_{ij} \end{bmatrix} \leq \begin{bmatrix} 0 \\ \Delta T \\ 0 \\ \Delta T \end{bmatrix} \quad \forall i, j \\ A_6 \mathbf{y} \leq \mathbf{b}_6. \end{gathered} \tag{27}$$

The next step is to use k_{ij}^{start} and k_{ij}^{end} to compute three sets of binary vectors, denoted $\mathbf{g}_{ij}^{\text{start}}$, $\mathbf{g}_{ij}^{\text{on}}$, and $\mathbf{g}_{ij}^{\text{end}}$, which act as selectors for indices which correspond to charge times. The values in $\mathbf{g}_{ij}^{\text{start}}$ and $\mathbf{g}_{ij}^{\text{end}}$ are equal to 1 during intervals that contain energy from the remainders r_{ij}^{start} and r_{ij}^{end}. For example, the values for $\mathbf{g}_{ij}^{\text{start}}$ and $\mathbf{g}_{ij}^{\text{end}}$ from the scenario in Fig. 7b would be

$$\mathbf{g}_{ij}^{\text{start}} = \begin{bmatrix} 1 \\ 0 \\ 0 \\ 0 \end{bmatrix} \text{ and } \mathbf{g}_{ij}^{\text{end}} = \begin{bmatrix} 0 \\ 0 \\ 1 \\ 0 \end{bmatrix}. \tag{28}$$

The values in $\mathbf{g}_{ij}^{\text{on}}$ will be equal to 1 for all time indices where buses charges the entire time. For example, the values in g_{ij}^{on} that correspond to Fig. 7b would be

$$\mathbf{g}_{ij}^{\text{on}} = \begin{bmatrix} 0 \\ 1 \\ 0 \\ 0 \end{bmatrix}. \tag{29}$$

Let $\mathbf{f}$ be a vector of one-based integer indices such that $f_w = w \; \forall w \in (1, \text{nPoint})$, where nPoint is the desired number

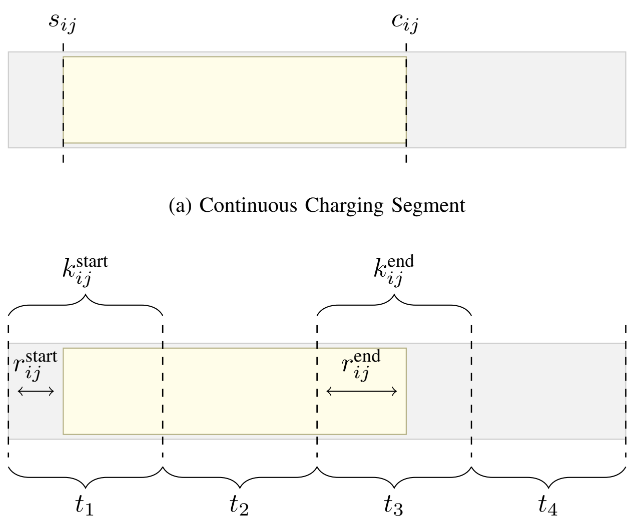

(b) Discrete Charging Segments

Fig. 7: Discretization of continuous charging intervals

of discrete samples. For example, if the day was discretized into 4 periods, then $\mathbf{f}$ would be

$$\mathbf{f} = \begin{bmatrix} 1 \\ 2 \\ 3 \\ 4 \end{bmatrix}. \tag{30}$$

Defining the index as an element of $\mathbf{f}$ allows us to convert from the single indices k_{ij}^{start} and k_{ij}^{end} to the binary vectors $\mathbf{g}_{ij}^{\text{start}}$ and $\mathbf{g}_{ij}^{\text{end}}$ by letting

$$\begin{aligned} k_{ij}^{\text{start}} &= \mathbf{f}^T \mathbf{g}_{ij}^{\text{start}} \\ k_{ij}^{\text{end}} &= \mathbf{f}^T \mathbf{g}_{ij}^{\text{end}} \\ 1 &= \mathbf{1}^T \mathbf{g}_{ij}^{\text{start}} \\ 1 &= \mathbf{1}^T \mathbf{g}_{ij}^{\text{end}} \\ \mathbf{g}_{ij}^{\text{start}} &\in \{0,1\}^{\text{nPoint}} \\ \mathbf{g}_{ij}^{\text{end}} &\in \{0,1\}^{\text{nPoint}}, \end{aligned} \tag{31}$$

which can be expressed in standard form and zero padded to form a set of linear constraints.

$$\begin{gathered} \begin{bmatrix} 0 & \mathbf{0}^T & -1 & \mathbf{f}^T \\ 0 & \mathbf{1}^T & 0 & 0 \\ -1 & \mathbf{f}^T & 0 & \mathbf{0}^T \\ 0 & 0 & 0 & \mathbf{1}^T \end{bmatrix} \begin{bmatrix} k_{ij}^{\text{start}} \\ \mathbf{g}_{ij}^{\text{start}} \\ k_{ij}^{\text{end}} \\ \mathbf{g}_{ij}^{\text{end}} \end{bmatrix} = \begin{bmatrix} 0 \\ 1 \\ 0 \\ 1 \end{bmatrix} \quad \forall i,j \\ \tilde{A}_3 \mathbf{y} = \tilde{\mathbf{b}}_3. \end{gathered} \tag{32}$$

The values of $\mathbf{g}_{ij}^{\text{on}}$ can be computed by first noticing that indices that correspond to complete charge intervals must remain between k_{ij}^{start} and k_{ij}^{end}, implying that

$$\left.\begin{aligned} g_w f_w &\leq k^{\text{end}} - 1 \\ g_w f_w &\geq k^{\text{start}} + 1 \end{aligned} \quad g_w = 1 \right\}, \tag{33}$$

which can be expressed as a set of linear constraints such that

$$\begin{aligned} g_w \cdot f_w &\leq k_{ij}^{\text{end}} + M(1 - g_w) - 1 \\ g_w \cdot f_w &\geq k_{ij}^{\text{start}} - M(1 - g_w) + 1 \end{aligned} \tag{34}$$

where M is $2 \cdot \text{nPoint}$. The constraints in (34) do not require that all values between k_{ij}^{start} and k_{ij}^{end} be set to one however, only that if a value is equal to one, that it must be between k_{ij}^{start} and k_{ij}^{end}. For all values between k_{ij}^{start} and k_{ij}^{end} to be 1, the sum of $\mathbf{g}_{ij}^{\text{on}}$ must be equal to the difference between k_{ij}^{end} and k_{ij}^{start} such that

$$\begin{aligned} g_w \cdot f_w &\leq k_{ij}^{\text{end}} + M(1 - g_w) - 1 \\ g_w \cdot f_w &\geq k_{ij}^{\text{start}} - M(1 - g_w) + 1 \\ \mathbf{1}^T \mathbf{g}_{ij}^{\text{on}} &= k_{ij}^{\text{end}} - k_{ij}^{\text{start}} - 1. \end{aligned} \tag{35}$$

The constraints in (35) work well for a general use case, however when k_{ij}^{end} is equal to k_{ij}^{start}, the last constraint in equation (35) becomes

$$\mathbf{1}^T \mathbf{g}_{ij}^{\text{on}} = -1 \tag{36}$$

which leads to an empty feasible set because all the elements of $\mathbf{g}_{ij}^{\text{on}}$ are binary. Let k_{ij}^{eq} be a binary variable which is equal to 0 when k_{ij}^{end} is not equal to k_{ij}^{start}. Equation (35) can be modified to incorporate k_{ij}^{eq} to switch between the cases where k_{ij}^{end} is equal, and not equal to k_{ij}^{start} by letting

$$\begin{aligned} g_w \cdot f_w &\leq k_{ij}^{\text{end}} + M(1 - g_w) - 1 \\ g_w \cdot f_w &\geq k_{ij}^{\text{start}} - M(1 - g_w) + 1 \\ \mathbf{1}^T \mathbf{g}_{ij}^{\text{on}} &= k_{ij}^{\text{end}} - k_{ij}^{\text{start}} - k_{ij}^{\text{eq}}. \end{aligned} \tag{37}$$

and constraining k_{ij}^{eq} such that

$$\begin{aligned} k_{ij}^{\text{end}} - k_{ij}^{\text{start}} - M k_{ij}^{\text{eq}} &\leq 0 \\ -k_{ij}^{\text{end}} + k_{ij}^{\text{start}} + M k_{ij}^{\text{eq}} &\leq M. \end{aligned} \tag{38}$$

The constraints from (37) and (38) can be expressed in standard form as

$$\begin{aligned} \mathbf{1}^T \mathbf{g}_{ij}^{\text{on}} - k_{ij}^{\text{end}} + k_{ij}^{\text{start}} + k_{ij}^{\text{eq}} &= 0 \\ k_{ij}^{\text{end}} - k_{ij}^{\text{start}} - M k_{ij}^{\text{eq}} &\leq 0 \\ -k_{ij}^{\text{end}} + k_{ij}^{\text{start}} + M k_{ij}^{\text{eq}} &\leq M \\ g_w \left(f_w + M\right) - k_{ij}^{\text{end}} &\leq M - 1 \\ g_w \left(M - f_w\right) + k_{ij}^{\text{start}} &\leq M - 1. \end{aligned} \tag{39}$$

The inequality constriants from equation (39) imply that

$$\begin{bmatrix} f_w + M & -1 & 0 \\ M - f_w & 0 & 1 \end{bmatrix} \begin{bmatrix} g_w \\ k_{ij}^{\text{end}} \\ k_{ij}^{\text{start}} \end{bmatrix} \leq \begin{bmatrix} M - 1 \\ M - 1 \end{bmatrix} \forall g_w \in \mathbf{g}_{ij}^{\text{on}} \tag{40}$$

and that

$$\begin{bmatrix} 1 & -1 & -M \\ -1 & 1 & M \end{bmatrix} \begin{bmatrix} k_{ij}^{\text{end}} \\ k_{ij}^{\text{start}} \\ k_{ij}^{\text{eq}} \end{bmatrix} \leq \begin{bmatrix} 0 \\ M \end{bmatrix} \quad \forall i,j, \tag{41}$$

which can be concatenated for all i, j and zero padded to form a joint matrix, satisfying

$$A_7 \mathbf{y} \leq \mathbf{b}_7. \tag{42}$$

Similarly, the equality constraint from equation (39) can also be concatenated and zero padded such that

$$\begin{gathered}\mathbf{1}^T\mathbf{g}_{ij}^{\text{on}} - k_{ij}^{\text{end}} + k_{ij}^{\text{start}} + k_{ij}^{\text{eq}} = 0 \ \forall i,j \\ \begin{bmatrix}\mathbf{1}^T & -1 & 1 & -1\end{bmatrix}\begin{bmatrix}\mathbf{g}_{ij}^{\text{on}} \\ k_{ij}^{\text{end}} \\ k_{ij}^{\text{start}} \\ k_{ij}^{\text{eq}}\end{bmatrix} = 0 \\ \tilde{A}_4\mathbf{y} = \tilde{\mathbf{b}}_4.\end{gathered} \tag{43}$$

The next step is to define the average power during intervals that only charge for part of the time. These intervals correspond to the remainder values r_{ij}^{start} and r_{ij}^{end} and, as with previous constraints, maintain different behavior when $k_{ij}^{\text{eq}} = 0$ and $k_{ij}^{\text{eq}} = 1$. The average power that corresponds to r_{ij}^{start} and r_{ij}^{end} can be computed as

$$\left.\begin{array}{ll} p_{ij}^{\text{start}} = \dfrac{p\cdot(\Delta T - r_{ij}^{\text{start}})}{\Delta T} & \\ p_{ij}^{\text{end}} = \dfrac{p\cdot r_{ij}^{\text{end}}}{\Delta T}. & k_{ij}^{\text{eq}} = 1 \\ & \\ p_{ij}^{\text{start}} = \dfrac{p\cdot\left(r_{ij}^{\text{end}} - r_{ij}^{\text{start}}\right)}{\Delta T} & k_{ij}^{\text{eq}} = 0 \\ p_{ij}^{\text{end}} = 0 & \end{array}\right\}. \tag{44}$$

Equation (44) can also be expressed as a set of linear inequality constraints such that

$$\begin{aligned} p_{ij}^{\text{start}} &\leq p - \frac{p}{\Delta T}r_{ij}^{\text{start}} + M\left(1 - k_{ij}^{\text{eq}}\right) \\ p_{ij}^{\text{start}} &\geq p - \frac{p}{\Delta T}r_{ij}^{\text{start}} - M\left(1 - k_{ij}^{\text{eq}}\right) \\ p_{ij}^{\text{start}} &\leq \frac{p}{\Delta T}r_{ij}^{\text{end}} - \frac{p}{\Delta T}r_{ij}^{\text{start}} + Mk_{ij}^{\text{eq}} \\ p_{ij}^{\text{start}} &\geq \frac{p}{\Delta T}r_{ij}^{\text{end}} - \frac{p}{\Delta T}r_{ij}^{\text{start}} - Mk_{ij}^{\text{eq}} \\ p_{ij}^{\text{end}} &\leq \frac{p}{\Delta T}r_{ij}^{\text{end}} + M\left(1 - k_{ij}^{\text{eq}}\right) \\ p_{ij}^{\text{end}} &\geq \frac{p}{\Delta T}r_{ij}^{\text{end}} - M\left(1 - k_{ij}^{\text{eq}}\right) \\ p_{ij}^{\text{end}} &\leq Mk_{ij}^{\text{eq}} \\ p_{ij}^{\text{end}} &\geq -Mk_{ij}^{\text{eq}}, \end{aligned} \tag{45}$$

where M is the battery capacity, and can be expressed in standard form as

$$\begin{aligned} p_{ij}^{\text{start}} + \frac{p}{\Delta T}r_{ij}^{\text{start}} + Mk_{ij}^{\text{eq}} &\leq M + p \\ -p_{ij}^{\text{start}} - \frac{p}{\Delta T}r_{ij}^{\text{start}} + Mk_{ij}^{\text{eq}} &\leq M - p \\ p_{ij}^{\text{start}} - \frac{p}{\Delta T}r_{ij}^{\text{end}} + \frac{p}{\Delta T}r_{ij}^{\text{start}} - Mk_{ij}^{\text{eq}} &\leq 0 \\ -p_{ij}^{\text{start}} + \frac{p}{\Delta T}r_{ij}^{\text{end}} - \frac{p}{\Delta T}r_{ij}^{\text{start}} - Mk_{ij}^{\text{eq}} &\leq 0 \\ p_{ij}^{\text{end}} - \frac{p}{\Delta T}r_{ij}^{\text{end}} + Mk_{ij}^{\text{eq}} &\leq M \\ -p_{ij}^{\text{end}} + \frac{p}{\Delta T}r_{ij}^{\text{end}} + Mk_{ij}^{\text{eq}} &\leq M \\ p_{ij}^{\text{end}} - Mk_{ij}^{\text{eq}} &\leq 0 \\ -p_{ij}^{\text{end}} - Mk_{ij}^{\text{eq}} &\leq 0 \end{aligned} \tag{46}$$

and by using matrix multiplication such that

$$\begin{gathered}\begin{bmatrix} 1 & 0 & \frac{p}{\Delta T} & 0 & M \\ -1 & 0 & -\frac{p}{\Delta T} & 0 & M \\ 1 & 0 & \frac{p}{\Delta T} & -\frac{p}{\Delta T} & -M \\ -1 & 0 & -\frac{p}{\Delta T} & \frac{p}{\Delta T} & -M \\ 0 & 1 & 0 & -\frac{p}{\Delta T} & M \\ 0 & -1 & 0 & \frac{p}{\Delta T} & M \\ 0 & 1 & 0 & 0 & -M \\ 0 & -1 & 0 & 0 & -M \end{bmatrix}\begin{bmatrix} p_{ij}^{\text{start}} \\ p_{ij}^{\text{end}} \\ r_{ij}^{\text{start}} \\ r_{ij}^{\text{end}} \\ k_{ij}^{\text{eq}} \end{bmatrix} \leq \begin{bmatrix} M+p \\ M-p \\ 0 \\ 0 \\ M \\ M \\ 0 \\ 0 \end{bmatrix} \ \forall i,j \\ A_8 \leq \mathbf{b}_8 \end{gathered} \tag{47}$$

where p_{ij}^{start}, p_{ij}^{end}, and p represent the average power that corresponds to r_{ij}^{start}, r_{ij}^{end}, and full charging intervals respectively. The total average power use is calculated as

$$\mathbf{p}_{\text{total}} = \bar{\mathbf{p}}_{\text{load}} + \sum_{ij}\mathbf{g}_{ij}^{\text{start}}\cdot p_{ij}^{\text{start}} + \mathbf{g}_{ij}^{\text{on}}\cdot p + \mathbf{g}_{ij}^{\text{end}}\cdot p_{ij}^{\text{end}} \tag{48}$$

where $\bar{\mathbf{p}}_{\text{load}}$ is the average power of the uncontrolled loads.

Note, however that (48) contains the bilinear terms $\mathbf{g}_{ij}^{\text{start}} \cdot p_{ij}^{\text{start}}$ and $\mathbf{g}_{ij}^{\text{end}} \cdot p_{ij}^{\text{end}}$. The expression $\mathbf{g}_{ij}^{\text{start}} \cdot p_{ij}^{\text{start}}$ from (48) can be thought of as a vector, $\mathbf{p}_{ij}^{\text{start}}$ which contains values for p_{ij}^{start} whenever g_{ij}^{start} is not equal to 0 such that

$$\left.\begin{array}{ll} p_w = p^{\text{start}} & g_w = 1 \\ p_w = 0 & g_w = 0 \end{array}\right\} \forall p_w \in \mathbf{p}_{ij}^{\text{start}}, \tag{49}$$

which can be rewritten as a set of linear inequality constraints such that

$$\begin{aligned} p_w &\geq p_{ij}^{\text{start}} - M(1-g_w)\forall p_w \in \mathbf{p}_{ij}^{\text{start}} \\ p_w &\leq p_{ij}^{\text{start}} + M(1-g_w)\forall p_w \in \mathbf{p}_{ij}^{\text{start}} \\ p_w &\geq -Mg_w\forall p_w \in \mathbf{p}_{ij}^{\text{start}} \\ p_w &\leq Mg_w\forall p_w \in \mathbf{p}_{ij}^{\text{start}} \end{aligned} \tag{50}$$

The same approach can be taken to replace $\mathbf{g}_{ij}^{\text{end}} \cdot p_{ij}^{\text{end}}$ with the vector $\mathbf{p}_{ij}^{\text{end}}$ by letting

$$\begin{aligned} p_w &\geq p_{ij}^{\text{end}} - M(1-g_w) \ \forall p_w \in \mathbf{p}_{ij}^{\text{end}} \\ p_w &\leq p_{ij}^{\text{end}} + M(1-g_w) \ \forall p_w \in \mathbf{p}_{ij}^{\text{end}} \\ p_w &\geq -Mg_w \ \forall p_w \in \mathbf{p}_{ij}^{\text{end}} \\ p_w &\leq Mg_w \ \forall p_w \in \mathbf{p}_{ij}^{\text{end}}, \end{aligned} \tag{51}$$

which can be written in standard form, stacked to accomodate the constraints for all i, j, and zero padded in the usual fashion as

$$\begin{gathered}\begin{bmatrix} -1 & 1 & M \\ 1 & -1 & M \\ -1 & 0 & -M \\ 1 & 0 & -M \end{bmatrix}\begin{bmatrix} p_w \\ p_{ij}^{\text{start}} \\ g_w \end{bmatrix} \leq \begin{bmatrix} M \\ M \\ 0 \\ 0 \end{bmatrix} \ \forall p_w \in \mathbf{p}_{ij}^{\text{start}} \\ A_9 \leq \mathbf{b}_9. \end{gathered} \tag{52}$$

Equation (51) can be expressed in standard form, stacked for all i, j, and zero padded in a similar fashion such that

$$\begin{gathered}\begin{bmatrix} -1 & 1 & M \\ 1 & -1 & M \\ -1 & 0 & -M \\ 1 & 0 & -M \end{bmatrix}\begin{bmatrix} p_w \\ p_{ij}^{\text{end}} \\ g_w \end{bmatrix} \leq \begin{bmatrix} M \\ M \\ 0 \\ 0 \end{bmatrix} \ \forall p_w \in \mathbf{p}_{ij}^{\text{end}} \\ A_{10}\mathbf{y} \leq \mathbf{b}_{10}. \end{gathered} \tag{53}$$

	On-Peak	Off-Peak	Both
Energy	On-Peak Energy Charge	Off-Peak Energy Charge	None
Energy Rate	$u_{\text{e-on}}$	$u_{\text{e-off}}$	None
Power	Demand Charge	None	Facilities Charge
Power Rate	$u_{\text{p-on}}$	None	$u_{\text{p-all}}$

Fig. 8: Description of the assumed billing structure

An expression for the total power used can then be expressed as

$$\mathbf{p}^{\text{total}} = \mathbf{p}^{\text{load}} + \sum_{ij} \mathbf{p}_{ij}^{\text{start}} + \mathbf{p}_{ij}^{\text{end}} + \mathbf{g}_{ij}^{\text{on}} \cdot p \tag{54}$$

and in standard form as

$$\begin{gathered} \begin{bmatrix} 1 & -1^{\text{start}} & -1^{\text{end}} & -1^{\text{on}} \cdot p \end{bmatrix} \begin{bmatrix} \mathbf{p}_w^{\text{total}} \\ \mathbf{p}_w^{\text{start}} \\ \mathbf{p}_w^{\text{end}} \\ \mathbf{g}_w^{\text{on}} \end{bmatrix} = \mathbf{p}_w^{\text{load}} \\ \tilde{A}_4 \mathbf{y} = \tilde{\mathbf{b}}_4 \end{gathered} \tag{55}$$

V. Objective Function

This work adopts the objective function developed in [19], which implements the rate schedule from [22]. The rate schedule in [22] is based off of two primary components: power and energy.

Power is billed per kW for the highest 15 minute average power over a fixed period of time. It is common practice for power providers to use a higher rate during "on-peak" periods when power is in higher demand and use a lower rate during "off-peak" hours, which account for all other time periods.

The rate schedule given in [22] assesses a fee for a users maximum average power during on-peak hours called the On-Peak Power charge, and a user's overall maximum average power, called a facilities charge as shown in figure 8.

Energy fees are also assessed per kWh of energy consumed with a higher rate for energy consumed during on-peak hours and a lower rate for energy consumed during off-peak hours.

A. Power Charges

It is necessary to compute the maximum power both overall and for on-peak periods. Section IV adopted the convention that ΔT denotes the time offset between power samples and that each power reading would reflect the average power used in the previous interval. Now let us set ΔT to 15 minutes, making $\mathbf{p}_{\text{total}}$ an expression of the 15 minute average power. Next, let $\mathcal{S}_{\text{on}}$ be the set of all indices belonging to on-peak time periods such that $j \in \mathcal{S}_{\text{on}}$ implies that the j^{th} element of $\mathbf{p}^{\text{total}}$, p_j^{total}, represents a 15 minute average during an on-peak interval and let q_{on} be the maximum on-peak average power. With these definitions, constriants for determining the maximum on-peak average are defined as

$$\begin{aligned} p_j^{\text{total}} &\le q_{\text{on}} \ \forall j \in \mathcal{S}_{\text{on}} \\ \begin{bmatrix} 1 & -1 \end{bmatrix} \begin{bmatrix} p_j^{\text{total}} \\ q_{\text{on}} \end{bmatrix} &\le 0 \ \forall j \in \mathcal{S}_{\text{on}} \\ A_{11} \mathbf{y} &\le \mathbf{0} \\ A_{11} \mathbf{y} &\le \mathbf{b}_{11} \end{aligned} \tag{56}$$

Because an increased value in q_{on} is directly related to an increase in cost, the optimizer will minimize q_{on} until it is equal to the maximum value in $\{p_j^{\text{total}} \ \forall j \in \mathcal{S}_{\text{on}}\}$. A similar proceedure can be used to derive a set of constraints for the overall maximum average power, denoted q_{all}, and is represented as

$$\begin{aligned} A_{12} \mathbf{y} &\le \mathbf{0} \\ A_{12} \mathbf{y} &\le \mathbf{b}_{12}. \end{aligned} \tag{57}$$

The charges for power are then expressed as

$$\begin{aligned} \text{power cost} &= q_{\text{on}} \cdot u_{\text{p-on}} + q_{\text{all}} \cdot u_{\text{p-all}} \\ &= \begin{bmatrix} u_{\text{p-on}} & u_{\text{p-all}} \end{bmatrix} \begin{bmatrix} q_{\text{on}} \\ q_{\text{all}} \end{bmatrix} \\ &= \mathbf{u}_{\text{p}}^T \mathbf{y} \end{aligned} \tag{58}$$

where $u_{\text{p-on}}$ is the rate per kW for on-peak power use, or the demand charge and $u_{\text{p-all}}$ is the rate per kW for the overall maximum 15 minute average.

B. Energy Charges

Energy is defined as the integral of power over a length of time. Because the values for power given in this work reflect an average power, the energy over a given period can be computed by multiplying the average power by the change in time, or ΔT such that

$$\text{Total Energy} = \mathbf{1}^T \mathbf{p}_{\text{total}} \cdot \Delta T. \tag{59}$$

However, because the energy is billed for on-peak and off-peak time periods, we define two binary vectors $\mathbf{1}_{\text{on}}$ and $\mathbf{1}_{\text{off}}$ such that $1_j^{\text{on}} = 1 \ \forall j \in S_{\text{on}}$ and zero otherwise. Similarly, $1_{\text{off}} = \mathbf{1} - 1_{\text{on}}$. The on-peak and off-peak energy can then be computed as

$$\begin{aligned} \text{On-Peak Energy} &= \mathbf{1}_{\text{on}}^T \mathbf{p}_{\text{total}} \cdot \Delta T \\ \text{Off-Peak Energy} &= \mathbf{1}_{\text{off}}^T \mathbf{p}_{\text{total}} \cdot \Delta T. \end{aligned} \tag{60}$$

Let $u_{\text{e-on}}$ and $u_{\text{e-off}}$ represent the on-peak and off-peak energy rates respectively. The total cost for energy is computed as

$$\begin{aligned} \text{Energy Cost} &= \left(\mathbf{1}_{\text{on}} \cdot u_{\text{e-on}} \cdot \Delta T\right)^T \mathbf{p}_{\text{total}} + \left(\mathbf{1}_{\text{off}} \cdot u_{\text{e-off}} \cdot \Delta T\right)^T \mathbf{p}_{\text{total}} \\ &= \left(\mathbf{u}_{\text{e-on}} + \mathbf{u}_{\text{e-off}}\right)^T \mathbf{p}_{\text{total}} \\ &= \mathbf{u}_{\text{e}}^T \mathbf{y} \end{aligned} \tag{61}$$

C. Cost Function and Final Problem

The entire cost function is given as the sum of the energy and power costs such that

$$\begin{aligned} \text{Cost} &= \mathbf{u}_{\text{p}}^T \mathbf{y} + \mathbf{u}_{\text{e}}^T \mathbf{y} \\ &= \left(\mathbf{u}_{\text{p}} + \mathbf{u}_{\text{e}}\right)^T \mathbf{y} \\ &= \mathbf{v}^T \mathbf{y} \end{aligned} \tag{62}$$

The complete problem can now be formulated as

$$\min_{\mathbf{y}} \mathbf{y}^T\mathbf{v} \text{ subject to}$$
$$\begin{bmatrix}\tilde{A}_1\\ \tilde{A}_2\\ \tilde{A}_3\end{bmatrix}\mathbf{y} = \begin{bmatrix}\tilde{\mathbf{b}}_1\\ \tilde{\mathbf{b}}_2\\ \tilde{\mathbf{b}}_3\end{bmatrix}, \quad \begin{bmatrix}A_1\\ A_2\\ A_3\\ A_4\\ A_5\\ A_6\\ A_7\\ A_8\\ A_9\\ A_{10}\\ A_{11}\\ A_{12}\end{bmatrix}\mathbf{y} \leq \begin{bmatrix}\mathbf{b}_1\\ \mathbf{b}_2\\ \mathbf{b}_3\\ \mathbf{b}_4\\ \mathbf{b}_5\\ \mathbf{b}_6\\ \mathbf{b}_7\\ \mathbf{b}_8\\ \mathbf{b}_9\\ \mathbf{b}_{10}\\ \mathbf{b}_{11}\\ \mathbf{b}_{12}\end{bmatrix} \tag{63}$$

or

$$\min_{\mathbf{y}} \mathbf{y}^T\mathbf{g} \text{ subject to}$$
$$\tilde{A}\mathbf{y} = \tilde{\mathbf{b}}, \; A\mathbf{y} \leq \mathbf{b}, \tag{64}$$

VI. Results

This section shows performance for the proposed bus charging algorithm and contains three subsections. Section VI-A describes the setup for the experiments. Section VI-B compares the proposed method with a previously published algorithm [11]. Section VI-C discusses the difference in computation time between prior work and the current method. TODO: include blurb in the beginning that talks about how the current discrete method lacks precision with large step size and is computationally difficult with small ones.

A. Setup

This section compares the monthly cost of energy for the proposed method with two other methods. The first method three different charge plans. The first charge plan follows a baseline algorithm which simulates how bus drivers at the Utah Transit Authority (UTA) in Salt Lake City (SLC) charge by default. The second charge plan is computed using the method in [11] which was selected because it is very similar to the proposed algorithm. Both the proposed method and the method in [11] use mixed integer linear programs to formulate a charge schedule and include time of day rates for energy.

Conversations with bus drivers at the UTA in SLC have shown that bus drivers generally top off their batteries whenever a charger is available which maximises the number of charge sessions in a day. Hence, the baseline algorithm follows the constraints in equation 63 but incentivizes buses to charge as frequently as possible. Let v_{σ}^{ijk} be the value of the objective function v at the index corresponding to σ_{ijk} from section II-B. By letting $v_{\sigma_{ijk}} = -1, \forall i, j, k$ and zero otherwise, the baseline effectively maximizes the number of times a bus can charge.

The comparisons in this section consider a 5 bus 5 charger scenario with a charge rate of 300 kW. Each solution is expressed in terms of a MILP and solved up to a 2% gap using Gurobi [10] unless otherwise specified. The uncontrolled loads from section IV are represented with a scaled version of historical data from the Trax Power SubStation at UTA.

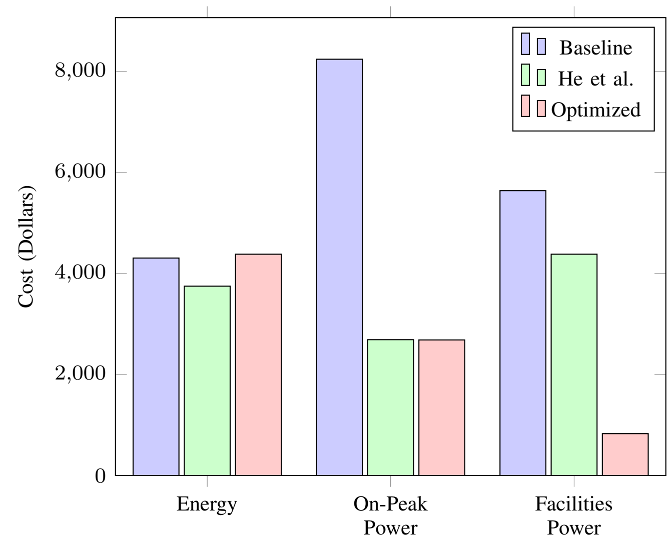

Fig. 9: Cost comparison with prior work

The scaling served to increase the difficulty of the charging problem and better illustrates the capabilities of our algorithm.

B. Cost Comparison with Prior Work

This section explores the differences in monthly cost between the charge schedules generated by three different algorithms including the baseline, results of [11], and our current work. All methods are evaluated according to the rate schedule in [22]. A comparison of all three algorithms is given in Fig. 9. Note how the cost of energy is generally the same for each algorithm and that the primary differences in cost come from come from the on-peak and facilities power charges, illustrating the need to minimize average peak power.

The difference in power management between the baseline and optimized algorithm is demonstrated in Fig. 10. Note how the optimized power profile is almost completely flat, indicating a steady power use, devoid of large spikes in the grid. In comparison, the baseline algorithm is less steady and includes periods of significant power use, leading to the increased power charges in Fig. 9.

The effect of uncontrolled loads on price is also demonstrated in Fig. 11. Note how the Optimized algorithm behaves inversely to the unconrolled loads, resulting in the flat load profile from Fig. 10. The load profile from [11] decreases the cost of energy by moving charge actions outside the on-peak period, however because it does not account for peak-related power costs, this movement comes at the expense of power chargers.

C. Computation Time

Up to this point, we have only considered algorithms that either charge at every opportunity or don't fully account for the entire rate schedule. This section shows a comparison of work by [19] which uses a network flow approach and discrete time axis to solve the charge problem. Because both the approach in [19] and the approach in this paper include the full rate schedule, their monthly costs are comparable.

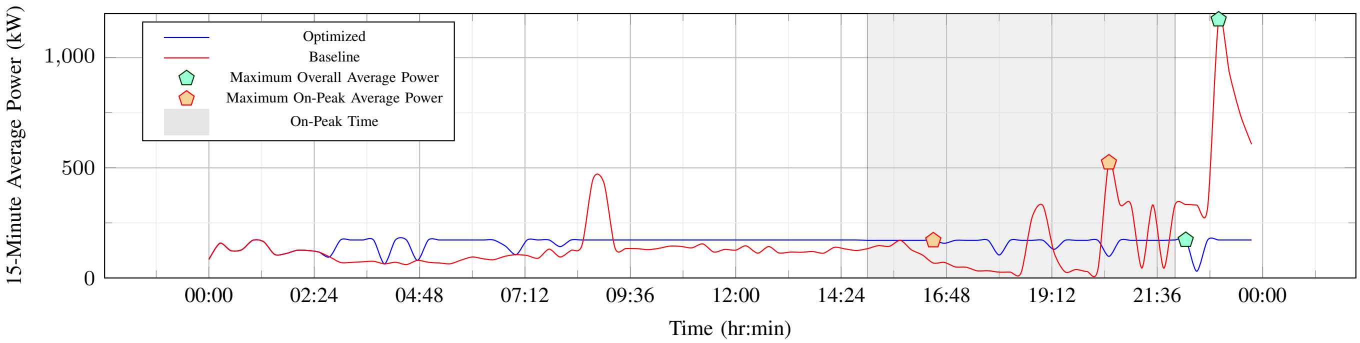

Fig. 10: 15-Minute average power for one day

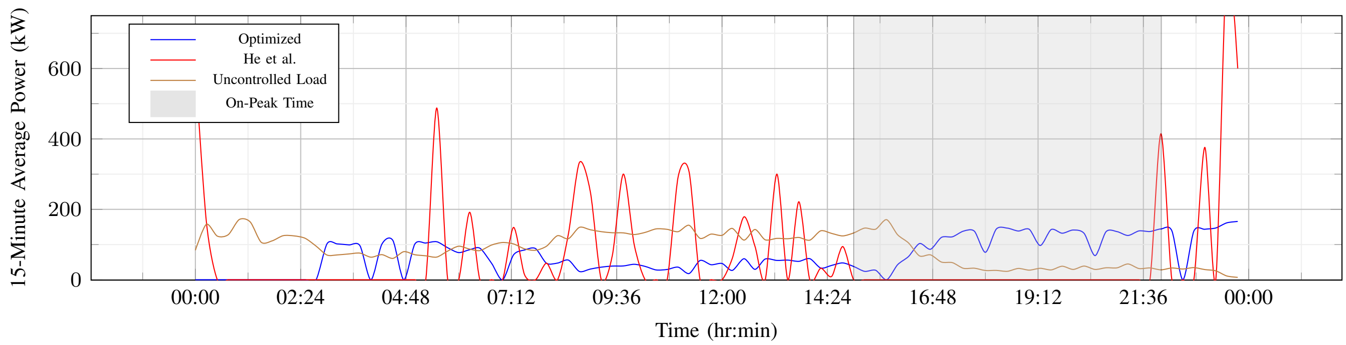

Fig. 11: Comparison between uncontrolled and bus loads

However, because the approach from [19] handles the time component discretely, higher fidelity time estimates become computationanlly prohibitive.

Fig. 12 compares the computation time for the proposed algorithm with [19] with a time step of one minute. The algorithms were run on a common desktop computer with 32 Gb of RAM and an 8 core 4 Gz processor and the method from [19] was solved up to a 5% gap. Note how the optimized algorithm is several orders of magnitude less to compute and gives the added benefit of floating point precision in its time estimates.

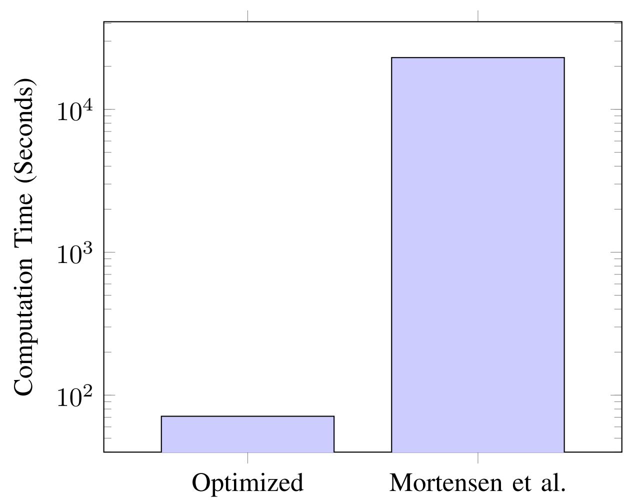

Fig. 12: Comparison of computation time between the proposed algorithm and [19]

VII. Conclusions and Future Work

In conclusions, the proposed algorithm yields significant cost savings over the work given in [11] and the baseline by decreases the 15-minute average power both overall and during on-peak periods. Additionally, time comparisons show that the proposed method offers high temporal resolution at no additional computational cost wheras the computations in prior work require several orders of magnitude more for a one minute time resolution.

Note that this work offers a framework for computing a globally optimal charge plan, however computational constraints render it unuseable for real-time updates. Future work might include approximate solutions from simpler hieristic approaches to reduce the computational complexity. Another approach could be to use additional methods that address real-time deviations by taking actions that best get back to the global plan.

Another known limitation includes how the computational complexity for the current method does not scale with large numbers of buses (more than 30). For larger bus fleets, a descentralized as opposed to a global method might work better.

Finally, this method does not account for uncertainty in the model. Stochastic events such as arrival times, deviations in uncontrolled loads, and battery discharge can significantly affect the useability of the global plan. There are techniques which account for uncertainty in similar frameworks which may be helpful in preventing unforeseen consequences.

References

[1] Poornesh et al. "A Comparative study on Electric Vehicle and Internal Combustion Engine Vehicles". In: *2020 Internat. Conf. on Smart Electronics and Communication*.

[2] Yaseen Alwesabi et al. "Robust strategic planning of dynamic wireless charging infrastructure for electric buses". In: *Applied Energy* (2022).

[3] Avishan Bagherinezhad et al. "Spatio-Temporal Electric Bus Charging Optimization With Transit Network Constraints". In: *IEEE Transactions on Industry Applications* (2020).

[4] Bhagyashree J Balde and Arghya Sardar. "Electric Road system With Dynamic Wireless charging of Electric buses". In: *IEEE Trans. Electrification Conf.* 2019.

[5] T. Boonraksa et al. "Impact of Electric Bus Charging on the Power Distribution System a Case Study IEEE 33 Bus Test System". In: *IEEE Grand Internat. Conf. and Exposition Asia*. 2019.

[6] Alexander Brown et al. "A Position Allocation Approach to the Scheduling of Battery Electric Bus Charging". In: (2020).

[7] Qifu Cheng et al. "A smart charging algorithm-based fast charging station with energy storage system-free". In: (2020).

[8] Bálint Csonka. "Optimization of Static and Dynamic Charging Infrastructure for Electric Buses". In: *Energies* (2021).

[9] Sanchari Deb, Karuna Kalita, and Pinakeshwar Mahanta. "Impact of electric vehicle charging stations on reliability of distribution network". In: *IEEE Internat. Conf. on Tech. Adv. in Power and Energy*. 2017.

[10] Gurobi Optimization, LLC. *Gurobi Optimizer Reference Manual*. 2022. URL: https://www.gurobi.com.

[11] Yi He, Ziqi Song, and Zhaocai Liu. "Fast-charging station deployment for battery electric bus systems considering electricity demand charges". In: *Sustainable Cities and Society* (2019).

[12] Adnane Houbbadi et al. "Optimal Charging Strategy to Minimize Electricity Cost and Prolong Battery Life of Electric Bus Fleet". In: *IEEE Vehicle Power and Propulsion Conf.* 2019.

[13] Shubham Jain et al. "Battery Swapping Technology". In: *IEEE Internat. Conf. on Recent Advances and Innovations in Engineering*. 2020.

[14] Seog Y. Jeong et al. "Automatic Current Control by Self-Inductance Variation for Dynamic Wireless EV Charging". In: *IEEE Workshop on Emerg. Tech.: Wireless Power Transfer*. June 2018.

[15] Hideki Kato et al. "Comparative measurements of the eco-driving effect between electric and internal combustion engine vehicles". In: *2013 World Electric Vehicle Symposium and Exhibition (EVS27)*. 2013.

[16] Rong-Ceng Leou and Jeng-Jiun Hung. "Optimal Charging Schedule Planning and Economic Analysis for Electric Bus Charging Stations". In: *Energies* (2017).

[17] Ning Ma and Zhili Zhou. "Mixed-integer Programming Model for Two-dimensional Non-guillotine Bin Packing Problem with Free Rotation". In: *Internat. Conf. for Information Science and Control Engineering*. 2017.

[18] Moataz Mahmoud et al. "Electric buses: A review of alternative powertrains". In: *Renewable and Sustainable Energy Reviews* (2016).

[19] Daniel Mortensen et al. "Comprehensive Cost Minimization for Charging Electric Bus Fleets". In: *IEEE Transactions on Intelligent Transportation Systems, In Review* (2021).

[20] Nanduni I. Nimalsiri et al. "A Survey of Algorithms for Distributed Charging Control of Electric Vehicles in Smart Grid". In: *IEEE Transactions on Intelligent Transportation Systems* (2020).

[21] Inaki Ojer et al. "Development of energy management strategies for the sizing of a fast charging station for electric buses". In: *IEEE International Conference on Environment and Electrical Engineering*. 2020.

[22] Rocky Mountain Power. *Rocky Mountain Power Electric Service Schedule No. 8*. 2021. URL: https://www.rockymountainpower.net/content/dam/pcorp/documents/en/rockymountainpower/rates-regulation/utah/rates/008_Large_General_Service_1_000_kW_and_Over_Distribution_Voltage.pdf.

[23] Nan Qin et al. "Numerical analysis of electric bus fast charging strategies for demand charge reduction". In: *Trans. Research Part A: Policy and Practice* (2016).

[24] Marco Rinalde et al. "Mixed-fleet single-terminal bus scheduling problem: Modeling, solution scheme and potential applications". In: *Omega* (2020).

[25] Xiaoxue Rong et al. "Coordinated charging strategy of electric vehicle charging station based on combination of linear power flow and genetic algorithm". In: *IEEE Asia-Pacific Power and Energy Engineering Conf.* 2016.

[26] Daniel Stahleder et al. "Impact Assessment of High Power Electric Bus Charging on Urban Distribution Grids". In: *IEEE Industrial Electronics Society*. 2019.

[27] Guang Wang et al. "BCharge: Data-Driven Real-Time Charging Scheduling for Large-Scale Electric Bus Fleets". In: *Proceedings - Real-Time Systems Symposium* (2019).

[28] Ran Wei et al. "Optimizing the spatio-temporal deployment of battery electric bus system". In: *Journal of Transport Geography* (2018).

[29] Justin Whitaker et al. "A Network Flow Approach to Battery Electric Bus Scheduling, in review". In: *IEEE Transactions on Intelligent Transportation Systems* (2022).

[30] Xian Zhang and Guibin Wang. "Optimal dispatch of electric vehicle batteries between battery swapping stations and charging stations". In: *IEEE Power and Energy Society General Meeting*. 2016.

[31] Yirong Zhou et al. "Bi-Objective Optimization for Battery Electric Bus Deployment Considering Cost and Environmental Equity". In: *IEEE Trans. on Intel. Transportation Systems* (2021).